Antimicrobial electrospun silver-, copper- and zinc-doped polyvinylpyrrolidone nanofibers

Please, cite as follows:

Jennifer Quirós, João P. Borges,Karina Boltes, Ismael Rodea-Palomares, Roberto Rosal, Antimicrobial electrospun silver-, copper- and zinc-doped polyvinylpyrrolidone nanofibers, Journal of Hazardous Materials, Volume 299, 15 December 2015, Pages 298-305, ISSN 0304-3894,

http://dx.doi.org/10.1016/j.jhazmat.2015.06.028

http://www.sciencedirect.com/science/article/pii/S0304389415004847

Antimicrobial electrospun silver-, copper- and zinc-doped polyvinylpyrrolidone nanofibers

Jennifer Quirós[1], João P. Borges[2], Karina Boltes[1,3], Ismael Rodea-Palomares[4], Roberto Rosal[1,3,*],

[1] Department of Chemical Engineering, University of Alcalá, 28871 Alcalá de Henares, Madrid, Spain
[2] CENIMAT/I3N, Departamento de Ciência dos Materiais, Faculdade de Ciências e Tecnologia, FCT, Universidade Nova de Lisboa, 2829-516 Caparica, Portugal
[3] Madrid Institute for Advanced Studies of Water (IMDEA Agua), Parque Científico Tecnológico, E-28805, Alcalá de Henares, Madrid, Spain
[4] Departamento de Biología, Facultad de Ciencias, Universidad Autónoma de Madrid, Cantoblanco, E-28049 Madrid, Spain

* Corresponding author: roberto.rosal@uah.es

Abstract

The use of electrospun polyvinylpyrrolidone (PVP) nanofibers containing silver, copper, and zinc nanoparticles was studied to prepare antimicrobial mats using silver and copper nitrates and zinc acetate as precursors. Silver became reduced during electrospinning and formed nanoparticles of several tens of nanometers. Silver nanoparticles and the insoluble forms of copper and zinc were dispersed using low molecular weight PVP as capping agent. High molecular weight PVP formed uniform fibers with a narrow distribution of diameters around 500 nm. The fibers were converted into an insoluble network using ultraviolet irradiation crosslinking. The efficiency of metal-loaded mats against the bacteria *Escherichia coli* and *Staphylococcus aureus* was tested for different metal loadings by measuring the inhibition of colony forming units and the staining with fluorescent probes for metabolic viability and compromised membranes. The assays included the culture in contact with mats and the direct staining of surface attached microorganisms. The results indicated a strong inhibition for silver-loaded fibers and the absence of significant amounts of viable but non-culturable microorganisms. Copper and zinc-loaded mats also decreased the metabolic activity and cell viability, although in a lesser extent. Metal-loaded fibers allowed the slow release of the soluble forms of the three metals.

Keywords: Electrospinning; Antibacterial; Polyvinylpyrrolidone; Nanoparticles

1. Introduction

The emergence of antimicrobial resistance is becoming a serious threat for the effective prevention and treatment of infections caused by bacteria, parasites, viruses, and fungi [1] and [2]. Novel antimicrobial agents are permanently sought to control infectious agents, which includes the design of novel antimicrobial compounds and drug-delivery vehicles [3] and [4]. It turns out that many pathogens of concern are able to attach to surfaces forming communities called biofilms. These are structured communities of bacterial cells enclosed in a self-produced polymeric matrix adhered to the surface [5]. Biofilm forming microorganisms benefit from an increased resistance against antimicrobials as well as the host organism's defense mechanisms, which make them particularly difficult to remove. In fact, microorganisms within biofilms dramatically increase the risk of disease transmission and the spreading of microorganisms causing spoilage or contamination of sensitive products such as food or pharmaceuticals as well as the cost of biofilm-control systems including mechanical or chemical cleaning [6].

Engineered membranes constitute a broad family of materials with a number of applications from biomedical to environmental fields. Membranes from nanofibrous materials are characterized by a high surface area to volume ratio, the presence of pores of bespoke sizes and their ease of functionalization [7]. Electrospinning is an efficient technique for the fabrication of polymer nanofibers, in which, under the influence of an electric field, a polymer solution or melt becomes fibers that get collected on a proper surface [8]. The technique is able to process mixtures of polymers or polymers carrying non-spinnable materials, so allowing a high degree of flexibility in the design of functional mats or membranes [9]. Electrospinning has been used to prepare nanofibrous scaffolds for gas and liquid filtration that benefits from adjustable functionality to prepare materials incorporating antimicrobial activity [10] and [11].

The incorporation of silver ions in membranes is a well-known way of enhancing their antibiofouling properties,

also acting as a safeguard in case some microorganisms reach the membrane surface [12] and [13]. The antibacterial and antifungal activity of silver, copper, and zinc has been extensively tested against a number of species [13] and [14]. A considerable discussion existed on whether the release or ion metals is or not the primary mechanism inhibiting microbial growth. Currently, it is generally accepted that the antibacterial and antifungal effect of metals in nanoparticle form is only partly explained by the interactions with released metal ions. For example, and concerning silver, it has been suggested that the mode of action of silver nanoparticles would comprise the damage to the structure of bacterial cell membranes and the depression of the activity of certain enzymes [15]. Metals in nanoparticle form present the advantage of acting as active reservoir, the case of silver being paradigmatic. Silver is toxic to bacteria due to its affinity to proteins and nucleic acids, but its ionic form is more prone than silver nanoparticles to be scavenged by organic matter or inorganic ligands in solution and therefore, nanoparticles would be an efficient vehicle for the delivery of metal to target organisms [16]. This approach has been used to prepare silver, copper, and zinc-doped methyltriethoxysilane coatings acting as metal reservoirs for antibacterial activity by Jaiswal et al. [17]. Fouda et al. used carboxymethyl chitosan as reducing agent for creating silver nanoparticles in a polyethylene oxide electrospun blend nano-fiber mats showing antimicrobial activity against several species of pathogenic and nonpathogenic microorganisms [18]. Several other polymer-based materials have been used to produce electrospun nanofibers containing silver nanoparticles, which include polyacrylonitrile (PAN) [19] and [20], PAN/titanium(IV) oxide composite (TiO2) [21], cellulose acetate [22] and [23], poly(N-vinylpyrrolidone) (PVP) [24], and poly(vinyl alcohol) [24], [25] and [26]. Among them PVP has the ability to produce electrospun fibers with large loads of inorganic ions and its ability to disperse particles acting as capping agent, which makes a polymer or choice for the fabrication of electrospun fibers with non-spinnable materials [27].

In this work, we studied the use of electrospun polyvinylpyrrolidone nanofibers containing silver, copper, and zinc nanoparticles obtained from their corresponding salts. The efficiency of metal-loaded mats against the bacteria *Escherichia coli* and *Staphylococcus aureus* was tested for different metal loadings.

2. Materials and methods

2.1 Materials

Low molecular weight polyvinylpyrrolidone, LMW–PVP, $(C_6H_9NO)_n$, 8000 g/mol, obtained from International Specialty Products (ISP) was used to prepare the sol–gel from which metal nanoparticles were produced. High molecular weight polyvinylpyrrolidone, HMW–PVP, 135,000 g/mol was purchased from Sigma–Aldrich and used as spinnable fiber for the electrospinning solutions with absolute ethanol as solvent. Silver nitrate ($AgNO_3$), copper(II) nitrate trihydrate ($Cu(NO_3)_2{\cdot}3H_2O$) and zinc acetate dihydrate ($ZnC_4H_6O_4{\cdot}2H_2O$) were obtained from Sigma–Aldrich. The components of culture media were biological grade acquired from Conda-Pronadisa (Spain). Fluorescein diacetate (FDA, CAS Number 596-09-8) and propidium iodide (PI, CAS Number 25535-16-4) were acquired from Sigma–Aldrich and used as cell viability stains. Live/Dead BacLight Bacterial Viability Kit was acquired from Molecular Probes Europe BV (Leiden, The Netherlands).

2.2 Electrospinning

Different concentrations of the salts $AgNO_3$, $Cu(NO_3)_2{\cdot}3H_2O$ and $(CH_3COO)_2Zn{\cdot}2H_2O$ were dissolved in absolute ethanol and then added drop wise to aqueous solutions of LMW PVP (14 wt.%, pH 7). The concentration of salts used were 3, 4, and 6 g of salt per 100 g of the solution of LMW–PVP. In what follows, these concentrations of metals are referred to as L, M, and H standing for low, medium, and high metal loadings. For higher loadings, the mats started to display defects such as beading and droplets. The details of compositions are included in Table S1 (Supporting information). In order to achieve complete dissolution and mixing, the sol was stirred for 2 h, after which the dispersing gels were available. The mixture for electrospinning was obtained by stirring for 2 h a mixture of HMW–PVP solution (14% wt.%, pH 7) and the dispersing gels prepared as indicated before in a 2:1 weight ratio. Their conductivity and viscosity are shown in Table S1 (Supporting information).

The electrospinning mixture was transferred to a 5 mL syringe with a 21-gauge stainless steel blunt-tip needle at its end. An infusion pump (KD scientific Series 100) controlled the solution flow. The needle and collector were connected to a high voltage power supply (Glassman DC high voltage power supply, EL series) in order to charge the polymer solution and create the required electric field between needle and collector. The collector used was a 1.9 × 5.5 cm aluminum grid separated 15 cm from the needle tip. The voltage used was 15 kV and the flow rate was 0.8 mL/h. After recovering the electrospun mats from the collector, they were dried for 24 h, after which a photo-crosslinking process was undertaken using the ultraviolet irradiation generated by the low pressure mercury lamps (254 nm) of a CL-1000 UV Crosslinker (UVP, Cambridge) operating with UV dose of 0.120 J/cm^2. The distance between the UV lamp and the electrospun mat was 8 cm and the irradiation was conducted at 25 ± 1 °C for 2 h. Photographs of crosslinked PVP in water and dried are provided in Fig. S1 (Supporting information).

2.3. Analytical methods

The morphological characterization of nanofibers was performed using scanning electron microscopy (SEM)

using a Zeiss DSM 962 apparatus. All samples for SEM were sputter-coated with gold before observation. Statistical diameter distributions were obtained from at least 50 measurements based on SEM images. Transmission electron microscopy (TEM) images were acquired in a JEOL JEM 2100 instrument. The conductivity and viscosity of electrospinning polymeric and precursor solutions was assessed using a conductivity meter (model HI 4521) from Hanna Instruments and a rotational rheometer Bohlin Gemini nano from Malvern Instruments equipped with 40 mm cone and plate fixtures respectively. Inductively coupled plasma-mass spectrometry analyses (ICP-MS) were performed on a NexION 300XX de PerkinElmer. Optical density (OD) was measured at 600 nm using a Shimadzu UV Spectrophotometer UV-1800. X-ray photoelectron spectroscopy (XPS) was carried out with a SPECS GmbH equipment equipped with ultra-high vacuum (10^{-10} mbar) and an energy analyzer PHOIBOS 150 9MCD. Fourier Transform InfraRed (FTIR) Nicolet iS50 from Thermo Scientific was used to analyze the surface of nanofibers. FTIR spectra of PVP fibers before and after irradiation are shown in Fig. S2 (Supporting information).

2.4. Microbial bioassays

The microorganisms used in this study were *E. coli* (CECT 516) and *S. aureus* (CECT 240). The strains are equivalent to ATCC 8739 and ATCC 6538P and were selected to comply with ISO 22,196 concerning the measurement of antibacterial activity on plastics surfaces. *E. coli* is a Gram-negative, facultative anaerobic, and rod-shaped bacterium commonly found in the lower intestine of warm-blooded organisms [28]. *E. coli* and other facultative anaerobes constitute about 0.1% of gut flora fecal–oral transmission being the major route for disease transmission [29]. Most *E. coli* strains are harmless, but some serotypes can cause serious health problems [30]. *S. aureus* is a Gram-positive coccal bacterium frequently found in human respiratory tract and on the skin. Although *S. aureus* is not always pathogenic, it is a common cause of skin infections, respiratory disease, and food poisoning. The microorganisms were preserved at −80° C in glycerol (20% v/v) until use. Reactivation was performed by culturing them in 50 mL Erlenmeyer's flasks and tracked by measuring OD at 600 nm. Both were grown at 30 °C, and kept in a rotary shaker at 150 min^{-1} during 24 h, after which they were in the stationary growth phase. The culture medium used was, for 1 L solution in distilled water: beef extract 5 g, peptone 10 g, NaCl 5 g and, for solid media, agar powder 15 g. pH was adjusted to 7.2. For each sample, 3 mL of the growth medium diluted to approximately 6×10^8 cell/mL was transferred to a Petri dish in contact with the electrospun mat and kept in a rotary shaker at 150 min^{-1} and 30 °C.

Bacterial viability was tested using fluorescein diacetate (FDA). Non-fluorescent FDA is transformed by active esterases in fully functional cells to yield the green-fluorescent compound fluorescein. The liquid fraction of cultures in contact with mats for 20 h at 30 °C was analyzed by taking an aliquot of 195 μL, which was transferred to 96-well microplates with 5 μL of FDA (0.02% w/w in in dimethyl sulfoxide). Fluorescence was measured using a fluorometer/luminometer Synergy HT-multi-mode microplate reader (Biotek, USA) in which FDA was excited at 485/20 nm, and its emission recorded at 528/20 nm. The incubation time for staining was 15 min at 25 °C.

Samples from the supernatant liquid in contact with mats were also taken to carry out bacterial plate counts. The antimicrobial activity of the studied mats was assessed based on the inhibition of colony forming units of exposed organisms. The colony forming assay was a miniaturization of the procedure described in ISO 22,196 based on Sieuwerts et al. [31]. Basically, aliquots of exposed organisms were diluted (8 serial dilutions, factor = 10) in phosphate saline medium were placed in sterile 96 well microtitter plates using an adjustable spacer multi-channel pipet (Pipet-Lite XLS, RAININ, USA). 4 Mini-spots of 10 μL per dilution were carefully dispensed on standard 50 mm Petri dishes containing standard rich agar-medium described in ISO 22,196. Plates were dried for 10 min. in sterile conditions and incubated for 24 h at 37 °C. Colony Forming Units (CFUs) were counted using a colony counting instrument CL-1110 (Acequilabs, Spain). For colony number estimations, at least four replicates of at least two serial dilutions in the plates were counted for each treatment. General appearance of the formed spots and colonies can be found in Fig. S3 (Supporting information). Estimations of CFU mL^{-1} were calculated according to the equation: CFU (cells mL^{-1}) = (n/V) Dil, where n = number of colonies, V = spot volumen (10 μL), Dil = dilution factor. A summary of the performance of the miniaturized method respect to the classical colony counting procedure can be found in Table S2 (Supporting information).

Live/Dead BacLight Bacterial Viability Kit (Molecular Probes, Invitrogen Detection Technologies, Carlsbad, CA, USA) was also used to visualize the viability of bacterial strains in contact with mats. The micrographs were obtained using a Leica Microsystems Confocal SP5 fluorescence microscope. In this staining system, viable cells exhibit green fluorescence (SYTO 9), whereas nonviable bacterial cells display red fluorescence (PI). PI is a red-fluorescent chromosome stain that marks dead cells as it is not permeant to undamaged membranes. The overlap of green and red appeared yellow. For mat staining, the whole surface of each mat was covered with BacLight stain (a mixture of SYTO 9 and PI in DMSO, according to manufacturer's recommendations) using 10 $\mu L/cm^2$ of the staining mixture. The incubation was performed during 15 min in the dark at room temperature. After incubation, 1 cm^2 of each mat was transferred to a glass slide, covered with a glass cover

slip and sealed. For green fluorescence (STYTO 9, live cells), the excitation was performed at 488 nm (Ar) and emission was recorded at 500–575 nm. For red fluorescence (PI, dead cells), the excitation/emission wavelengths were 561 nm (He–Ne) and 570–620 nm, respectively.

The presence of non-viable cells on mats was quantitatively assessed by performing direct readings of fluorescence intensity on different points over the surface of metal-loaded and unloaded mats, which corresponded to microorganisms attached to it after removing the culture medium. The mats for it were cut into 15 mm diameter circles and fixed on 24-well-multidishes (Black Visiplate™ TC, Wallac), every well containing as support agar powder (20 g/L) in distillated water. 66 μL of growth medium diluted to approximately 6×10^8 cell/mL was carefully extended over the whole mat surface. The measurements were taken using the microplate reader indicated before during the exponential phase growth of bacteria, approximately 6 h after inoculation, using 10 μL of PI (0.02% w/w in dimethyl sulfoxide), which were distributed on the surface of mats. PI excitation and emission wavelengths were 590/20 and 645/40, respectively. The incubation time for staining was 15 min at 25 °C. Details on the experimental setup and the surface mapping procedure can be found elsewhere [32].

3. Results

3.1. Preparation of composites mats

Crosslinking provided stability the mats. UV irradiation is known to promote the photolysis of pyrrolidone groups with the generation of macroradicals, the recombination of which gives rise to polymer crosslinking [33]. Mats after being recovered from electrospinning collector are shown in Fig. S4 (Supporting information) and after photocrosslinking in Fig. S5 (Supporting information, left column). The contact of fibers with water produces nanofibrous hydrogels with a high swelling degree due to water absorption [34] and [35]. Irradiated mats lose 36.2 ± 3.1% of their weight after 24 h in contact with water, which corresponded essentially with the LMW–PVP, the remaining being a backbone of HMW–PVP that remained water insoluble and displayed no evident flaws in fibers as shown in the confocal micrograph of a PVP wet fiber shown in Fig. S6 (Supporting information). Fig. S5 (Supporting information, right column) shows SEM micrographs of fibers immersed in water until constant weight and subsequently dried for SEM. In what follows, washed preconditioned mats were used, either neat or metal-loaded, for the experimental results reported in what follows. These mats displayed a weight loss <5% in all cases. Fiber diameters were determined from SEM images with at least 50 measurements per metal and concentration. The electrospun mats obtained displayed a narrow range of fiber diameters in all cases. No significant differences were found for fibers containing different metal loadings (L, M, and H) or for different metals: Ag: 464 ± 43 nm, Cu 495 ± 51 nm, and Zn 452 ± 48 nm. SEM images of mats prepared with the three Ag, Cu, and Zn loadings are shown in Fig. S4 (Supporting information). Fig. 1 shows TEM images of the three types of fibers. The presence of silver nanoparticles of a few tens of nanometers is apparent. In fact, the formation of silver nanoparticles began prior to the UV irradiation and was due to the reducing action of PVP itself, which converts silver ions into metallic silver: after putting in contact silver salt and LMW–PVP a darkening of the suspension was immediately observed due to the formation silver nanoparticles [36]. The process was further enhanced by the photo-reduction process of remaining silver ions as a result of UV irradiation [37]. Low molecular weight PVP has been shown to acts as size controller and dispersant during the formation of nanoparticles from copper salts because it hinders the nuclei from aggregation through the polar groups, which absorb copper particles on the surface with coordination bonds [38]. Copper salt was mixed with PVP in the absence of specific reducing agents, so the solid phase formed was a mixture of the different Cu(II) species that are oversaturated under the specific conditions used in this work, namely $Cu(OH)_2$, $Cu_2(OH)_3NO_3$, and CuO. The speciation of dissolved species was obtained using visual MINTEQ (version 3.1, KTH, Stockholm, Sweden), which is a model that uses a thermodynamic database to determine the equilibrium distribution of various species in aqueous solution. Concerning zinc, the insoluble species precipitating at the working pH were ZnO and $Zn(OH)_2$. Again, PVP worked as size controller and polymeric capping agent. The synthesis of colloidal solutions of zinc oxide using PVP as stabilizer has been assessed elsewhere [39]. The in-situ synthesis of Cu/Zn nanofibers has been also undertaken by Wu et al. [40] using PVP as polymer precursor for the preparation of crystalline ceramic fibers.

The presence of metal within the fibers has also been assessed using XPS as indicated in Fig. S7 (Supporting information). The XPS spectrum of pure neat PVP fibers is shown in Fig. S7A with the characteristic peaks from O1s, N1s, and C1s. Ag $3d_{5/2}$ and Ag $3d_{3/2}$ binding energies in the spectrum of Ag–PVP appear at 367.3 and 373.3 eV, respectively. The Ag $3d_{5/2}$ at 367.3 eV corresponds to silver oxide (Fig. S7B). It was not possible to determine the species because binding energies for Ag_2O and AgO are quite similar. The broadening of 367.3 eV the peak towards higher and lower energies corresponds to metallic silver and to the silver bonded to the organic capping agent as indicated elsewhere [41]. Concerning copper composites (Fig. S7C) the peak of $2p_{3/2}$ appears at 932.3 eV, the Cu(II) oxidation state being revealed by the peak at 943.0 eV. No intensity was observed in the zone of 919 eV reported to the position of metallic copper [42]. This fact and the lack of evidence for an overlapping of several peaks at 932.3 eV led us to conclude that all the copper was as Cu(II), either oxide or hydroxide this being difficult to

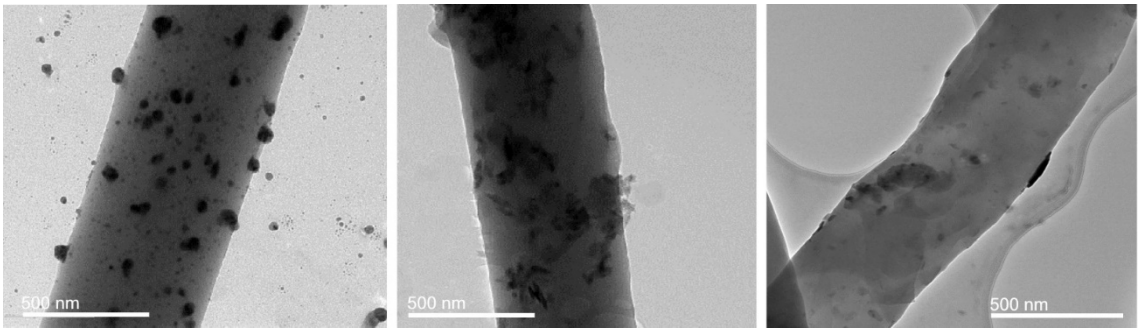

Figure 1. TEM micrographs of M-Ag-PVP (6.0 g Ag/100 g PVP, left), M-Cu-PVP (2.5 g Cu/100 g PVP, middle) and M-Zn-PVP (2.9 g Zn/100 g PVP, right).

assess due because binding energies are very similar [43]. Zinc signature appeared as $2p_{3/2}$ at 1021.5 and $2p_{1/2}$ 1044.5 eV peaks (Fig. S7D). Again, the absence of overlapping together with chemical considerations pointed towards Zn(II) species, probably a mixture of oxides and hydroxides.

Fig. 2 displays the amount of metal in mats in contact with the culture medium of microorganisms as described above (pH 7.2). The results in Fig. 2 are relative to the theoretical metal content of mats as produced and expressed in mass of metal per 100 g of LMW + HMW–PVP. The loss for zero time corresponds to metal washed off with during the stabilization process and was greater for Ag–PVP most probably as a consequence of the reduction process leading to reduced silver nanoparticles entrapped in LMW–PVP, the less tightly bound material more prone to become unattached from fibers during water conditioning. For the case of silver, there was also

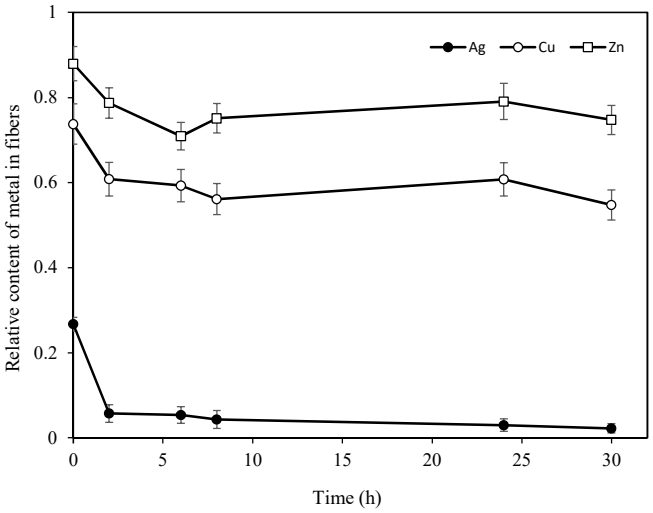

Figure 2. Metal content in fibers after exposure to culture medium for mats loaded with Ag (○), Cu (●) and Zn (□) prepared with 9.5 g of salt/100 g PVP (M-fibers).

observed a significant loss of metal during the first 2 h in contact with culture medium. Using MINTEQ the speciation of dissolved metal, once the mat reached a hypothetical equilibrium with the culture medium, indicated that most silver (>90% of dissolved silver) passed to the solution forming $AgCl_2^-$ and $AgCl_3^{2-}$, a speciation facilitated by the high amount of chloride ion in the culture medium and the reason for the rapid leaching of silver [44]. Concerning copper, the species in solution were $Cu_2(OH)_2^{2+}$, $Cu_3(OH)_4^{2+}$, and Cu^{2+}, rather that chlorinated forms. Zinc, on the other hand, was predominantly as Zn^{2+} with a minor contribution of $ZnCl^+$, $Zn(CH_3COO)^+$, and other chlorinated and hydroxylated forms. For both copper and zinc, the loss of metal was statistically significant, but considerably lower than that of silver mats. In all cases there was a slight tendency to loose metal after the initial decay, but at a considerably lower rate.

3.2 Evaluation of mats for antibacterial performance

Fig. 3 shows the results of colony counting and bacterial viability measured using FDA for microorganisms recovered from the culture media in contact with mats after 20 h at 30 °C. The results are expressed as a ratio with pure PVP fibers and showed a clear inhibition of microorganisms in contact with all metal-loaded mats. This was particularly high for silver, ranging 70–90% for the three tested loadings. The results displayed no significant differences between CFU determined using the miniaturized method described before and FDA signal revealing cell viability and measured microplate reader. Confidence intervals overlap in most cases showing that there was no clear trend for any of the methods towards higher or lower values. These results indicated that, for the range of metal loadings used in this work, CFU did not led to systematically lower values, a bias which is associated to the presence of significant amounts of viable but non-culturable microorganisms [32].

The confocal micrographs of Fig. 4 show the results of Live/Dead BacLight Bacterial Viability Kit on neat and metal-loaded mats. The micrographs display the double staining (SYTO 9 and PI, green, and red respectively) which highlights viable (green) and membrane damaged (red) cells. The first column corresponds to *S. aureus* and the second to *E. coli*. The higher antibacterial effect of silver is apparent in Fig. 4C and D that show mat surfaces essentially free from microorganisms. Although the effect of silver for *S. aureus* seems to be higher than form *E. coli*, this is most probably due to the selection of pictures or the somewhat higher growth rate of the later.

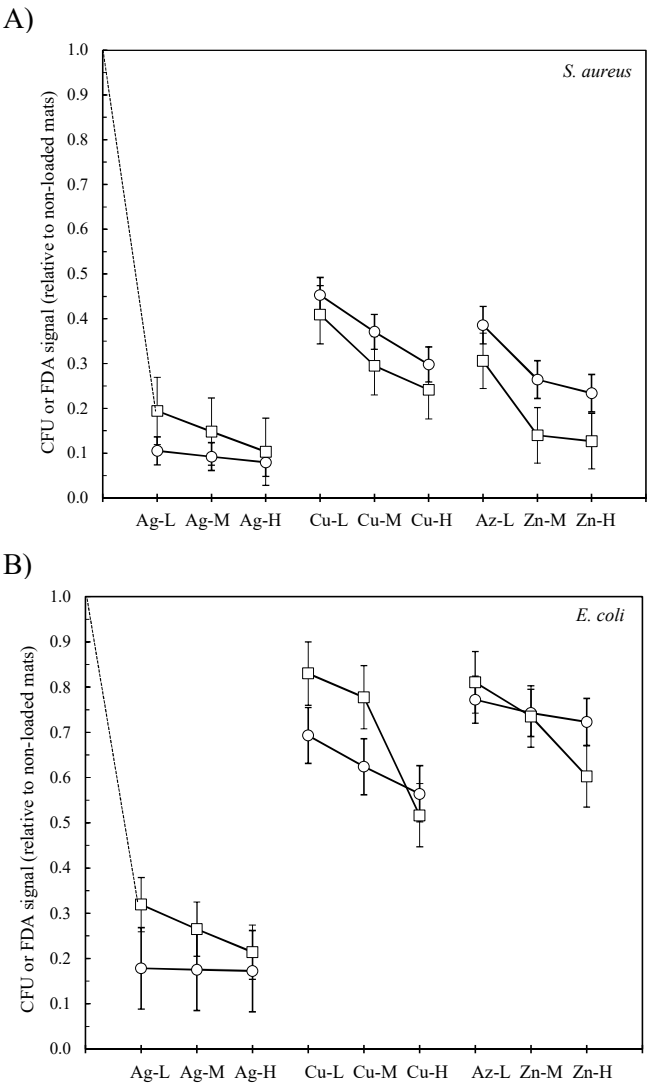

Figure 3. Colony forming units (○) and FDA signal (□) for mats in contact with *S. aureus* (A) and *E. coli* (B) with different metal loadings relative to neat fibers (1 = unloaded mats).

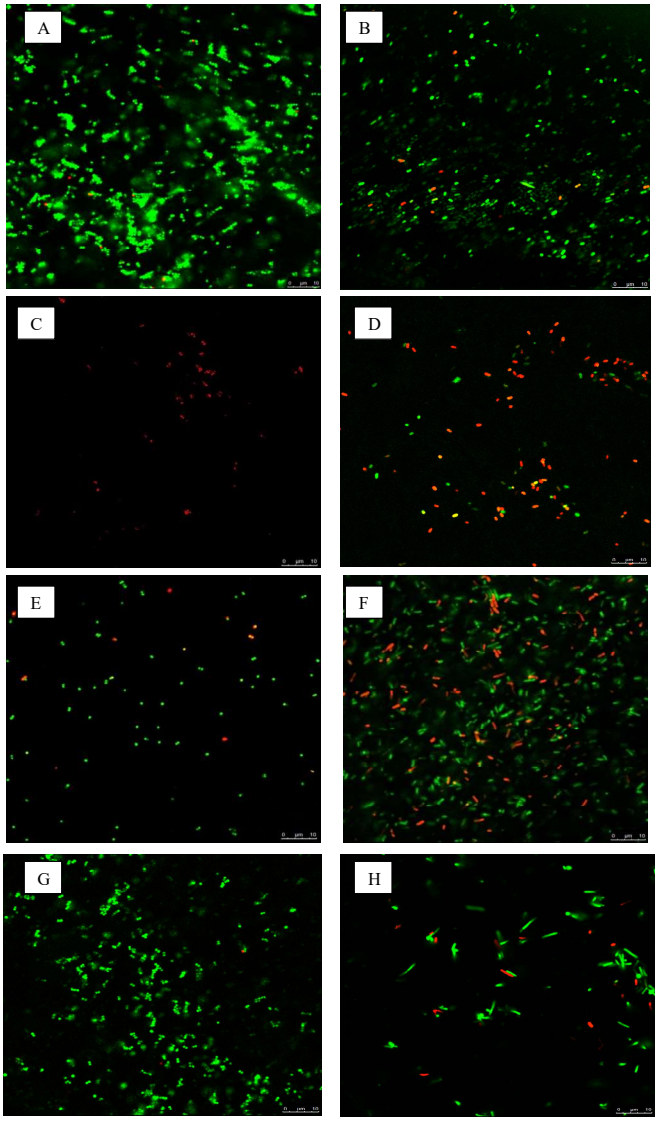

Figure 4. Live/Dead double staining of *S. aureus* on mats, PVP (A), PVP-Ag (C), PVP-Cu (E), PVP-Zn (G). *E. coli* on mats, PVP (B), PVP-Ag (D), PVP-Cu (F), PVP-Zn (H).

The images also display the presence of a higher number of red-stained non-viable cells on mats exposed to *E. coli*, rather than on those cultured with *S. aureus*. This can be explained by the differences between gram-positive *S. aureus* and gram-negative *E. coli*, which considerably differ in the structure of the envelope. Gram-positive bacteria have a thick peptidoglycan layer below the cell membrane that protects bacteria from external stresses and is believed to reduce the penetration of toxic substances. Due to it, the outer layer of Gram-negative bacteria allows higher permeation of low molecular weight substances, which is thought to make them more sensitive to toxics [45]. In practice, however, the differences are difficult to assess. For example, those concerning the tolerance to metals have been reported not significant elsewhere [46]. In order to better address this point, we performed a series of quantitative measurements of cell viability using PI directly on the surface of mats. The fluorescence emitted was measured in top mode, integrating the signal over time and for a surface mapping within the plate reader as indicated before.

Microplate simultaneous readings of PI are shown in Fig. 5 for mats cultured with *S. aureus* and *E. coli*. The signal is represented relative to non-loaded PVP and indicates, together with the corresponding confidence intervals, the increase in non-viable cells after 6 h of culture under metal-stressed conditions. The maximum amount of damaged cells corresponded to silver-loaded mats, with >50% increase of PI signal for the higher metal loadings. All data for loaded mats were statistically significant against the pure PVP mats except for zinc at its lowest metal content. The greater antimicrobial effect of silver for microorganisms in contact with mats agrees with the data taken from the supernatant and shown in Fig. 3. *S. aureus* displayed systematically higher PI values than *E. coli* but the differences were not statistically significant in any case. These results do not exclude differences in metabolic pathways. In fact, it has been shown that the internalization of metals can follow different mechanisms in Gram-negative and Gram-positive bacteria, but results are difficult to explain in part due to the fact, noted before, that metal can undergo an intricate speciation in

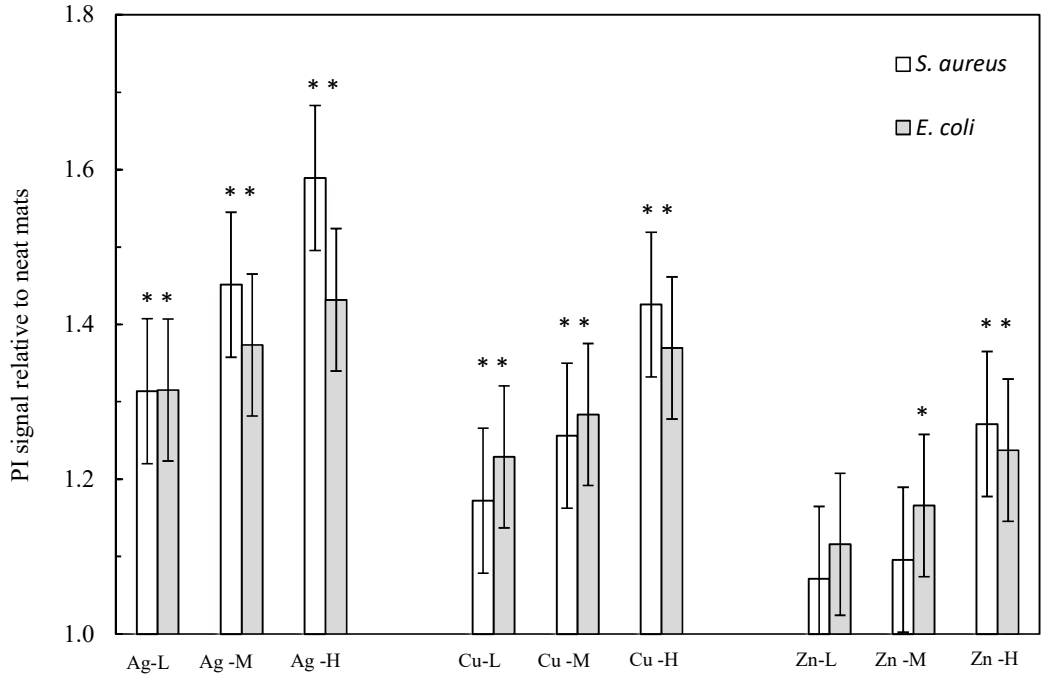

Figure 5. Non-viable cells on the surface of mats as stained with PI for *S. aureus* (white) and *E. coli* (shadowed). The signal is shown relative to non-metal loaded mats, after 6 h in contact with cultures (* = significant difference with respect to unloaded mats).

culture media [47]. In the presence of chloride, it has been shown that silver in solution is roughly 90% forming chlorinated species with a minor contribution of Ag^+. This speciation does not depend on pH and the content of silver ions in solution relates with chloride concentration [48]. The initial loss of silver of mats exposed to culture media was due to the pass of silver to the solution and was probably the reason for the high FDA and CFU inhibition observed in Fig. 3 for culture media in contact with mats. The biocidal effect persisted for measures taken on mats after 6 h with the remaining and slowly released silver as noted in Fig. 5. It is accepted that metals combine with the thiol groups of proteins leading to membrane damage and intracellular metabolic impairment [49] and [50]. The effect of nanoparticles is more controversial. It has been stated that silver nanoparticles generate reactive oxygen species (ROS) that damage bacterial DNA or mitochondria [51] and [52]. Although certain contribution from this mechanism cannot be excluded, the results shown here are consistent with a scenario in which loaded fibers act as reservoir in which the silver in nanoparticle form became captured so allowing the controlled release of dissolved metal. A similar reason is most probably behind the observed effect for copper and zinc, particularly for the latter. Zinc is a soluble metal, which according to the expected speciation would appear as Zn^{2+} (85%) and $ZnCl^+$ (10%), but the results showed that the insoluble forms do not give rise to a rapid dissolution of zinc. With copper, the situation was similar, although the insoluble forms of copper, CuO and the hydroxides $Cu(OH)_2$ and $Cu_2(OH)_3NO_3$ are less soluble than ZnO and $Zn(OH)_2$. Finally, it is interesting to note that all viability measurements have been performed in bacterial culture medium, which represents the most favourable growing conditions for them. Consequently, a much higher effect is expected under conditions less advantageous for microorganisms [53].

4. Conclusions

Silver, copper, and zinc were included in PVP composite nanofibers using electrospinning from solutions of their salt precursors. Low molecular weight PVP as size controller and polymeric capping agent. The mats, based on high molecular weight PVP and stabilized by ultraviolet irradiation, displayed a narrow distribution of diameters around 500 nm.

Silver was reduced during electrospinning giving rise to nanoparticles of several tens on nanometers, which became partially entrapped within the fiber network. Copper and zinc retained their oxidation state, but formed insoluble species including copper and zinc oxides and several hydroxides.

Metal-loaded mats were efficient against *E. coli* and *S. aureus* as tested by measuring the inhibition of CFU and the staining with FDA as viability marker. The results showed a strong inhibition for silver-loaded fibers and the absence of significant amounts of viable but non-culturable microorganisms.

The presence of damaged cells on mats was determined by the intensity of PI fluorescence on different points of their surface. All metal-loaded fibers displayed

antimicrobial effect, that of silver being particularly higher. There was little difference between *E. coli* and *S. aureus* concerning cell damage.

The results indicated that metal-loaded fibers acted as reservoir in which silver in nanoparticle form and copper and zinc as oxides or hydroxides became entrapped allowing the slow release of dissolved metal.

Acknowledgements

Financial support for this work was provided by FCT-MEC, Portugal, through UID/CTM/500025/2013 project, the FP7-ERA-Net Susfood, 2014/00153/001, the Spanish Ministry of Economy and Competitiveness, CTM2013-45775 and the Dirección General de Universidades e Investigación de la Comunidad de Madrid, Research Network S2013/MAE-2716. One of the authors, J.Q., thanks the University of Alcalá for the award of a pre-doctoral grant.

Appendix A. Supplementary data

Supplementary data related to this article can be found at http://www.sciencedirect.com/science/article/pii/S0304389415004847.

References

[1] Pfaller M.A. Antifungal drug resistance: mechanisms, epidemiology, and consequences for treatment. The American Journal of Medicine 125 (2012) S3-S13, 2012.

[2] Cantas L., Shah S.Q.A., Cavaco L.M., Manaia C.M., Walsh F., Popowska M., Garelick H., Bürgmann H., Sørum H. A brief multi-disciplinary review on antimicrobial resistance in medicine and its linkage to the global environmental microbiota. Front. Microbiol. 4 (2013) 96, doi: 10.3389/fmicb.2013.00096, eCollection 2013

[3] Singh, S. Nanomedicine–nanoscale drugs and delivery systems. J. Nanosci. Nanotechno. 10 (2010) 7906-7918.

[4] Villa, T. G., Veiga-Crespo, Antimicrobial Compounds: Current Strategies and New Alternatives. Springer Berlin-Heidelberg, 2014.

[5] Costerton, J.W., Stewart, P.S., Greenberg, E.P. Bacterial biofilms: a common cause of persistent infections. Science 284 (1999) 1318-1322.

[6] Chmielewski, R.A.N., Frank, J.F. Biofilm formation and control in food processing facilities. Compr. Rev. Food Sci. Food Saf. 2 (2003) 22-32.

[7] Balamurugan, R., Sundarrajan, S., Ramakrishna, S. Recent trends in nanofibrous membranes and their suitability for air and water filtrations. Membranes 1 (2011) 232-248.

[8] Huang, H.H., Ni, X.P., Loy, G.L., Chew, C.H., Tan, K.L., Loh, F.C., Deng, J.F., Xu, G.Q. Photochemical Formation of Silver Nanoparticles in Poly(N-vinylpyrrolidone). Langmuir 12 (1996) 909–912.

[9] Dasari, A., Quirós, J., Herrero, B., Boltes, K., García-Calvo, E., Rosal, R. Antifouling membranes prepared by electrospinning polylactic acid containing biocidal nanoparticles. J. Memb. Sci. 405 (2012) 134-140.

[10] Yoon, K., Hsiao, B.S., Chu, B., Functional nanofibers for environmental applications. J. Mater. Chem. 18 (2008) 5326-5334.

[11] dos Santos, R., Rocha, Â., Matias, A., Duarte, C., Sá-Nogueira, I., Lourenço, N., Borges, J.P., Vidinha, P. Development of antimicrobial Ion Jelly fibers. RSC Adv. 3 (2013) 24400-24405.

[12] Jung, R., Kim, Y., Kim, H.S., Jin, H.J. Antimicrobial properties of hydrated cellulose membranes with silver nanoparticles. J. Biomat. Sci. Polym. Ed. 20 (2009) 311-324.

[13] Lemire, J.A., Harrison, J.J., Turner, R.J. Antimicrobial activity of metals: mechanisms, molecular targets and applications. Nat. Rev. Microbiol. 11 (2013) 371-384.

[14] Malachová, K., Praus, P., Rybková, Z., Kozák, O. Antibacterial and antifungal activities of silver, copper and zinc montmorillonites. Appl. Clay Sci. 53 (2011) 642-645.

[15] Li, W.R., Xie, X.B., Shi, Q.S., Zeng, H.Y., Yang, Y.S., Chen, Y.B. Antibacterial activity and mechanism of silver nanoparticles on *Escherichia coli*. Appl. Microbiol. Biotechnol. 85 (2010) 1115-1122.

[16] Kang, F., Alvarez, P.J., Zhu D., Nanoparticles and Antagonize Bactericidal Activity. Environ. Sci. Technol. 48 (2014) 316–322.

[17] Jaiswal, S., McHale, P., Duffy, B. Preparation and rapid analysis of antibacterial silver, copper and zinc doped sol–gel surfaces. Colloids Surf. B: Biointerfaces 94 (2012) 170-176.

[18] Fouda, M.M.G., El-Aassar, M.R., Al-Deyab, S.S. Antimicrobial activity of carboxymethyl chitosan/polyethylene oxide nanofibers embedded silver nanoparticles, Carbohydr. Polym. 92, (2013) 1012-1017.

[19] Yang, Q.B., Li, D.M., Hong, Y.L., Li, Z.Y., Wang, C., Qiu, S.L., Wei, Y. Preparation and characterization of a PAN nanofibre containing Ag nanoparticles via electrospinning. Synth. Met. 137 (2003) 973–974.

[20] Lee, H.K., Jeong, E.H., Baek, C.K., Youk, J.H. One-step preparation of ultrafine poly(acrylonitrile) fibers containing silver nanoparticles. Mater. Lett. 59 (2005) 2977–2980.

[21] Lim, S.K., Lee, S.K., Hwang, S.H., Kim, H. Photocatalytic deposition of silver nanoparticles onto organic/inorganic composite nanofibers. Macromol. Mater. Eng. 291 (2006) 1265–1270.

[22] Son, W.K., Youk, J.H., Lee, T.S., Park, W.H. Preparation of antimicrobial ultrafine cellulose acetate fibers with silver nanoparticles. Macromol. Rapid Commun. 25 (2004) 1632–1237.

[23] Son, W.K., Youk, J.H., Park, W.H. Antimicrobial cellulose acetate nanofibers containing silver nanoparticles. Carbohydr. Polym. 65 (2006) 430–434.
[24] Jin, W.J., Lee, H.K., Jeong, E.H., Park, W.H., Youk, J.H. Preparation of polymer nanofibers containing silver nanoparticles by using poly(N-vinylpyrrolidone). Macromol. Rapid Commun. 26 (2005) 1903–1907.
[25] Hong, K.H., Park, J.L., Sul, I.H., Youk, J.H., Kang, T.J. Preparation of antimicrobial poly(vinyl alcohol) nanofibers containing silver nanoparticles. J. Polym. Sci. Part B Polym. Phys. 44 (2006) 2468–2674.
[26] Hong, K.H. Preparation and properties of electrospun poly(vinyl alcohol)/silver fiber web as wound dressings. Polym. Eng. Sci. 47 (2007) 43–49.
[27] Chuangchote, S., Sagawa, T., Yoshikawa, S., Electrospinning of poly(vinyl pyrrolidone): Effects of solvents on electrospinnability for the fabrication of poly(p-phenylene vinylene) and TiO2 nanofibers. J. Appl. Polym. Sci. 114 (2009) 2777–2791.
[28] Singleton, P. Bacteria in Biology, Biotechnology and Medicine (5th ed.). Wiley, New York, 1999, pp. 444–454.
[29] Eckburg, P.B., Bik, E.M., Bernstein, C.N., Purdom, E., Dethlefsen, L., Sargent, M., Gill, S.R., Nelson, K.E., Relman, D.A. Diversity of the human intestinal microbial flora. Science 308 (2005) 1635–1638.
[30] Vogt, R.L., Dippold, L. *Escherichia coli* O157:H7 outbreak associated with consumption of ground beef, June–July 2002. Public Health Rep. 120 (2005) 174–178.
[31] Sieuwerts, S., De Bok, F.A.M., Mols, E., De Vos, W.M., Van Hylckama Vlieg, J.E.T. A simple and fast method for determining colony forming units. Lett. Appl. Microbiol. 47 (2008) 275–278.
[32] Quirós, J., Boltes, K., Aguado, S., Guzman, R. Vilatela, J.J., Rosal, R. Antimicrobial metal-organic frameworks incorporated into electrospun fibers. Chem. Eng. J. 262 (2015) 189–197.
[33] Lopergolo, L.C, Lugao, A.B., Catalani, L.H. Direct UV photocrosslinking of poly(N-vinyl-2-pyrrolidone) (PVP) to produce hydrogels. Polymer 44 (2003) 6217-6222.
[34] Lopérgolo, L.C., Lugão, A.B., and Catalani, L.H. Direct UV photocrosslinking of poly(*N*-vinyl-2-pyrrolidone) (PVP) to produce hydrogels. Polymer, 44, 6217–6222, 2003.
[35] Fogaça, R., Catalani, L.H. PVP hydrogel membranes produced by electrospinning for protein release devices. Soft Mater. 11, 61-68, 2013.
[36] Wang, H., Qiao, X., Chen, J., Wang, X., Ding, S., Mechanisms of PVP in the preparation of silver nanoparticles. Mater. Chem. Phys. 94 (2005) 449–453.
[37] Huang, Z.M., Zhang, Y.Z., Kotaki, M., Ramakrishna, S. A review on polymer nanofibers by electrospinning and their applications in nanocomposites. Compos. Sci. Technol. 63 (2003) 2223–2253.
[38] Yu, W., Xie, H., Chen, L., Li, Y., Zhang, C. Synthesis and Characterization of Monodispersed Copper Colloids in Polar Solvents. Nanoscale Res Lett. 4 (2009) 465–470.
[39] Gutul, T., Rusu, E., Condur, N., Ursaki, V., Goncearenco, E., Vlazan, P. Preparation of poly (N-vinylpyrrolidone)-stabilized ZnO colloid nanoparticles. Beilstein J. Nanotechnol. 5 (2014) 402-406.
[40] Wu, Y., Dong, Z., Jenness, N.J., Clark, R.L. In-situ formation of Cu metal crystals within nanostructured ZnO electrospun fibers, Mat. Lett. 65 (2011) 2683-2685.
[41] Sumesh, E., Bootharaju, M.S., Pradeep, A.T. A practical silver nanoparticle-based adsorbent for the removal of Hg^{2+} from water. J. Hazard. Mater. 189 (2011) 450–457.
[42] McIntyre, N.S., Sunder, S., Shoesmith, D.W., Stanchell, F.W., Chemical information from XPS - applications to the analysis of electrode surfaces. J. Vac. Sci. Technol. 18 (1981) 714-421.
[43] Biesinger, M.C., Lau, L.W.M., Gerson, A.R., Smar, R.S.C. Resolving surface chemical states in XPS analysis of first row transition metals, oxides and hydroxides: Sc, Ti, V, Cu and Zn. Appl. Surf. Sci. 257 (2010) 887–898.
[44] Levard, C., Mitra, S., Yang,T., Jew, A.D., Badireddy, A.P., Lowry, G.C., Brown, G.E. Effect of chloride on the dissolution rate of silver nanoparticles and toxicity to *E. coli*. Environ. Sci. Technol. 2013, (2013) 5738−5745.
[45] Madigan, M.T., Martinko, J.M., Dunlap, P.V., Clark, D.P. Biology of microorganisms. Pearson, New York, 2009, p. 1061.
[46] Yasuyuki, M., Kunihiro, K., Kurissery, S., Kanavillil, N., Sato, Y., Kikuchi, Y. Antibacterial properties of nine pure metals: a laboratory study using *Staphylococcus aureus* and *Escherichia coli*, Biofouling 26 (2010) 851-858.
[47] Nies, D.H. Microbial heavy-metal resistance. Appl. Microbiol. Biotechnol. 51 (1999) 730-750.
[48] Lin, Y.E., Vidic, R.D., Stout, J.E., Yu, V.L., Negative effect of high pH on biocidal efficacy of copper and silver ions in controlling *Legionella pneumophila*. Appl. Environ. Microbiol. 68 (2012) 2711–2715.
[49] Liau, S.Y., Read, D.C., Pugh, W.J., Furr, J.R., Russell, A.D. Interaction of silver nitrate with readily identifiable groups - relationship to the antibacterial action of silver ions. Lett. Appl. Microbiol. 25 (1997) 279-283.

[50] Jung, W.K., Koo, H.C., Kim, K.W., Shin, S., Kim, S.H., Park, Y.H. Antibacterial activity and mechanism of action of the silver ion in *Staphylococcus aureus* and *Escherichia coli*. Appl. Environ. Microbiol. 74 (2008) 2171–2178.

[51] Xu, H., Qu, F., Xu, H., Lai, W., Wang Y.A., Aguilar, Z.P., Wei, H. Role of reactive oxygen species in the antibacterial mechanism of silver nanoparticles on *Escherichia coli* O157:H7. Biometals 25 (2012) 45-53.

[52] Feng, Q.L., Wu, J., Chen, G.Q., Cui, F.Z., Kim, T.N., Kim, J.O. A mechanistic study of the antibacterial effect of silver ions on *Escherichia coli* and *Staphylococcus aureus*. J. Biomed. Mater. Res. A 52 (2000) 662–668, 2000.

[53] Horowitz, J., Normand, M.D., Corradini, M.G., Peleg, M. Probabilistic Model of Microbial Cell Growth, Division, and Mortality. Appl. Environ. Microbiol. 76 (2010) 230-242.

Supplementary Material

Antimicrobial electrospun silver-, copper- and zinc-doped polyvinylpyrrolidone nanofibers

Jennifer Quirós[a], João P. Borges[b], Karina Boltes[a,c], Ismael Rodea-Palomares[d], Roberto Rosal[a,c*]

[a] Department of Chemical Engineering, University of Alcalá, 28871 Alcalá de Henares, Madrid, Spain.

[b] CENIMAT/I3N, Departamento de Ciência dos Materiais, Faculdade de Ciências e Tecnologia, FCT, Universidade Nova de Lisboa, 2829-516 Caparica, Portugal.

[c] Madrid Institute for Advanced Studies of Water (IMDEA Agua), Parque Científico Tecnológico, E-28805, Alcalá de Henares, Madrid, Spain.

[d] Departamento de Biología, Facultad de Ciencias, Universidad Autónoma de Madrid, Cantoblanco, E-28049 Madrid, Spain

Contents:

Table S1. Properties of polymer solutions.

Metal and identification of specimens	grams of salt per 100 gram of PVP	grams of Ag, CuO and ZnO per 100 g of HMW-PVP	grams of Ag, CuO and ZnO per 100 g of mat	conductivity (μS/cm)	viscosity (Pa s)
L-Ag	7.14	6.80	6.37	173.5	0.107
M-Ag	9.52	9.07	8.32	237.5	0.113
H-Ag	14.3	13.6	12.0	287.0	0.101
L-Cu	7.14	3.53	3.41	102.5	0.083
M-Cu	9.52	4.71	4.50	142.5	0.087
H-ACu	14.3	7.06	6.60	167.1	0.096
L-Zn	7.14	4.00	3.85	13.9	0.104
M-Zn	9.52	5.34	5.07	17.3	0.099
H-Zn	14.3	8.02	7.42	20.0	0.100

Table S2. Comparison of the performance of classical and miniaturized colony counting assay.

Assay	Target inoculum	Estimated inoculum	SD Intra-experimental	SD Inter-experimental	C.V[1] (%)	n[2]
Classical	$6x10^5$	3.06×10^5	1.09×10^5	6.53×10^4	21	7
Mini	$6x10^5$	4.75×10^5	2.65×10^5	1.60×10^5	33	7

[1] Inter-experimental variation coefficient C.V. (%) = (SD/mean) x 100
[2] n = 7 independent experiments with at least 3 intra-experimental replicates

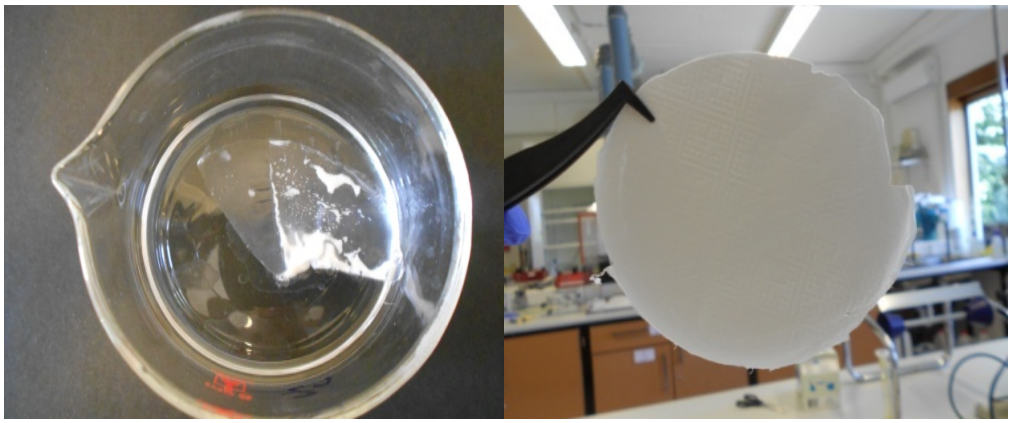

Fig. S1. Photographs of fibers in water after crosslinking (left) and dried PVP fibers (right)

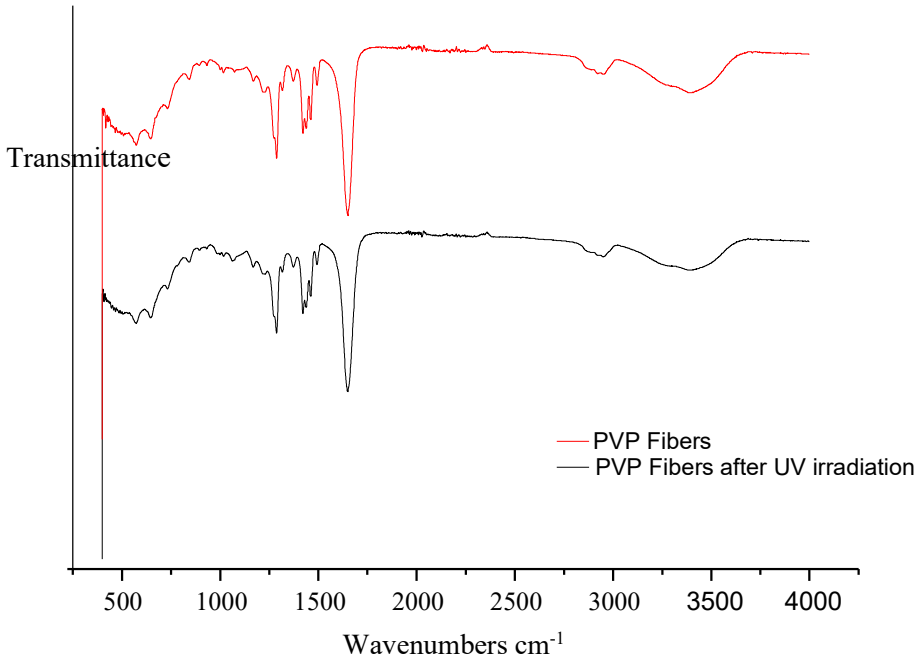

Fig. S2. FTIR spectrum of PVP fibers before and after UV crosslinking

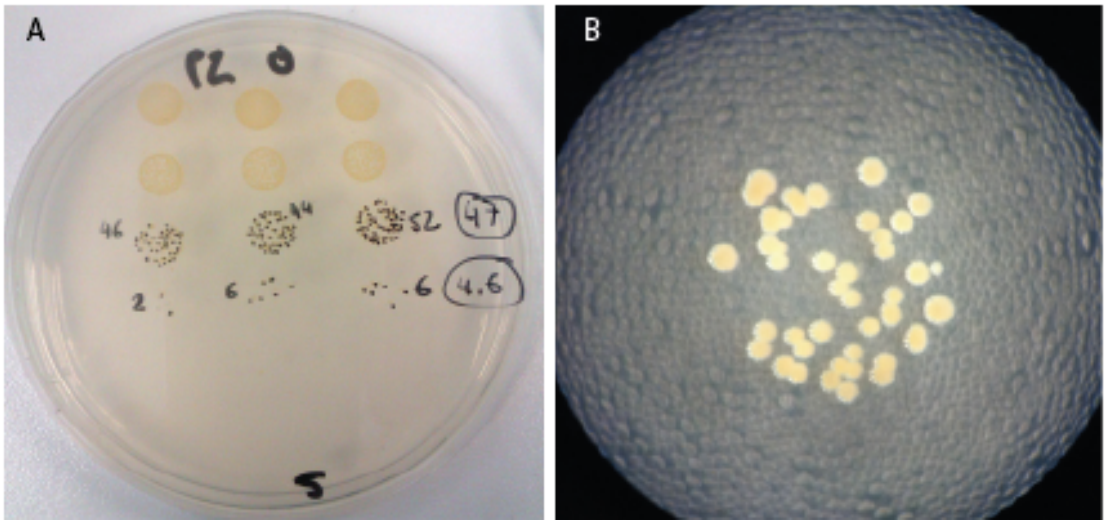

Fig. S3. (A) General appearance of mini-spot colony forming assay using *S. aureus*. (B) Detail of a typical 10^{-2} dilution of control *S. aureus* under a dissecting microscope (5 x magnification). As can be seen in the figure, individual CFUs can be reasonably counted in two serial dilutions.

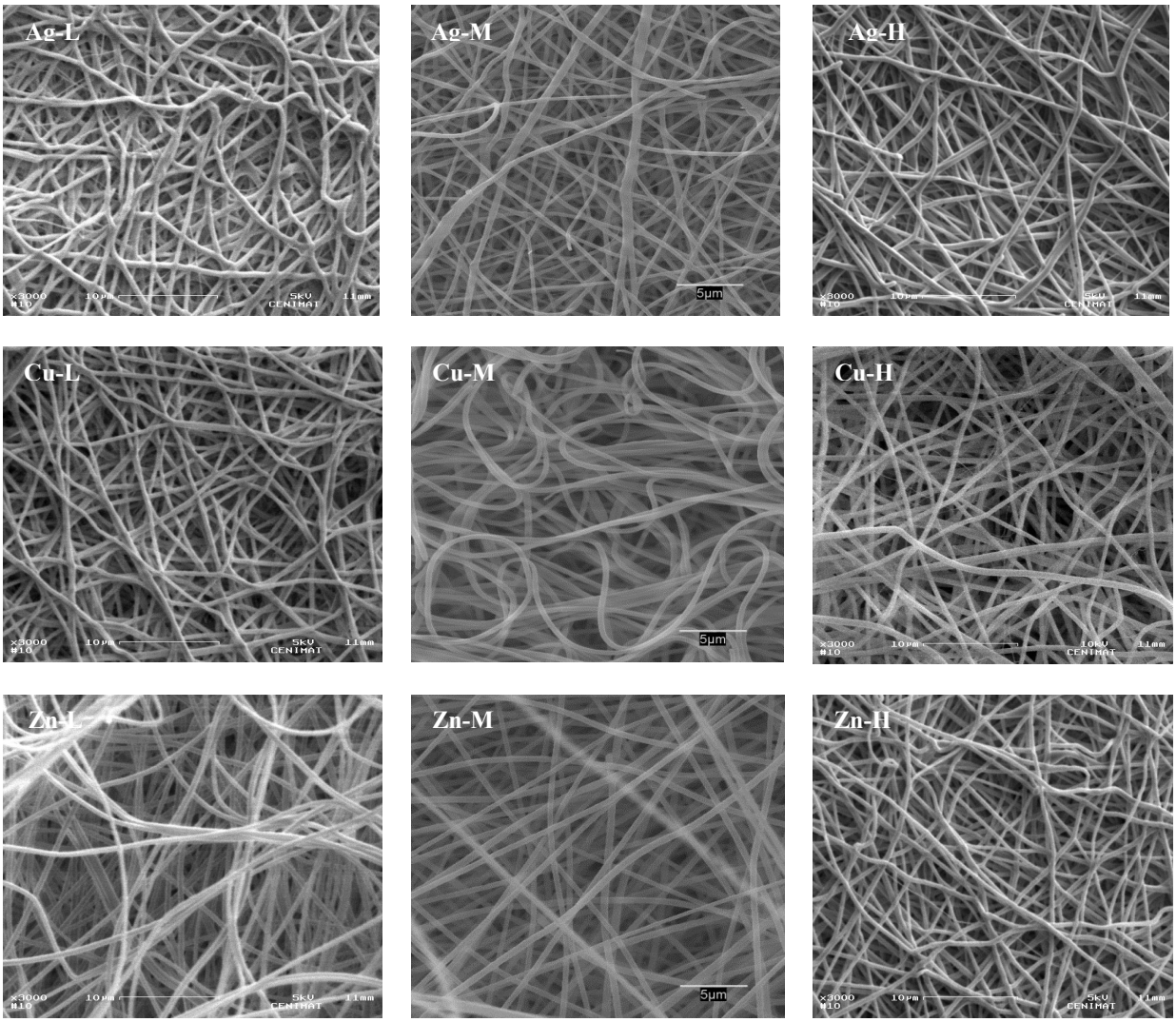

Fig. S4. SEM micrographs of silver (Ag), copper (Cu) and zinc (Zn) loaded PVP mats for the three concentrations, L, M and H.

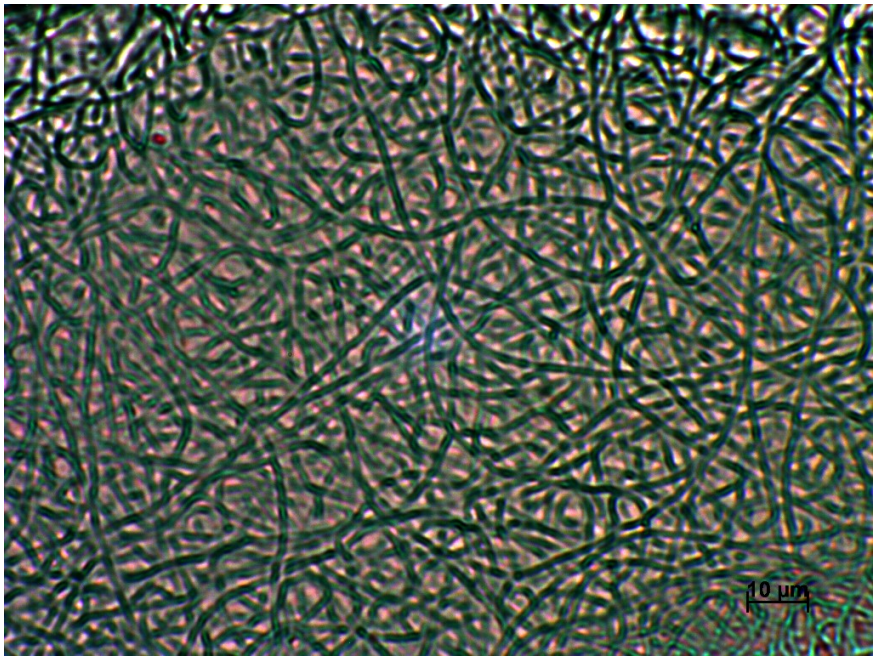

Fig. S5. Confocal micrograph of a UV-crosslinked PVP fiber after immersion in water

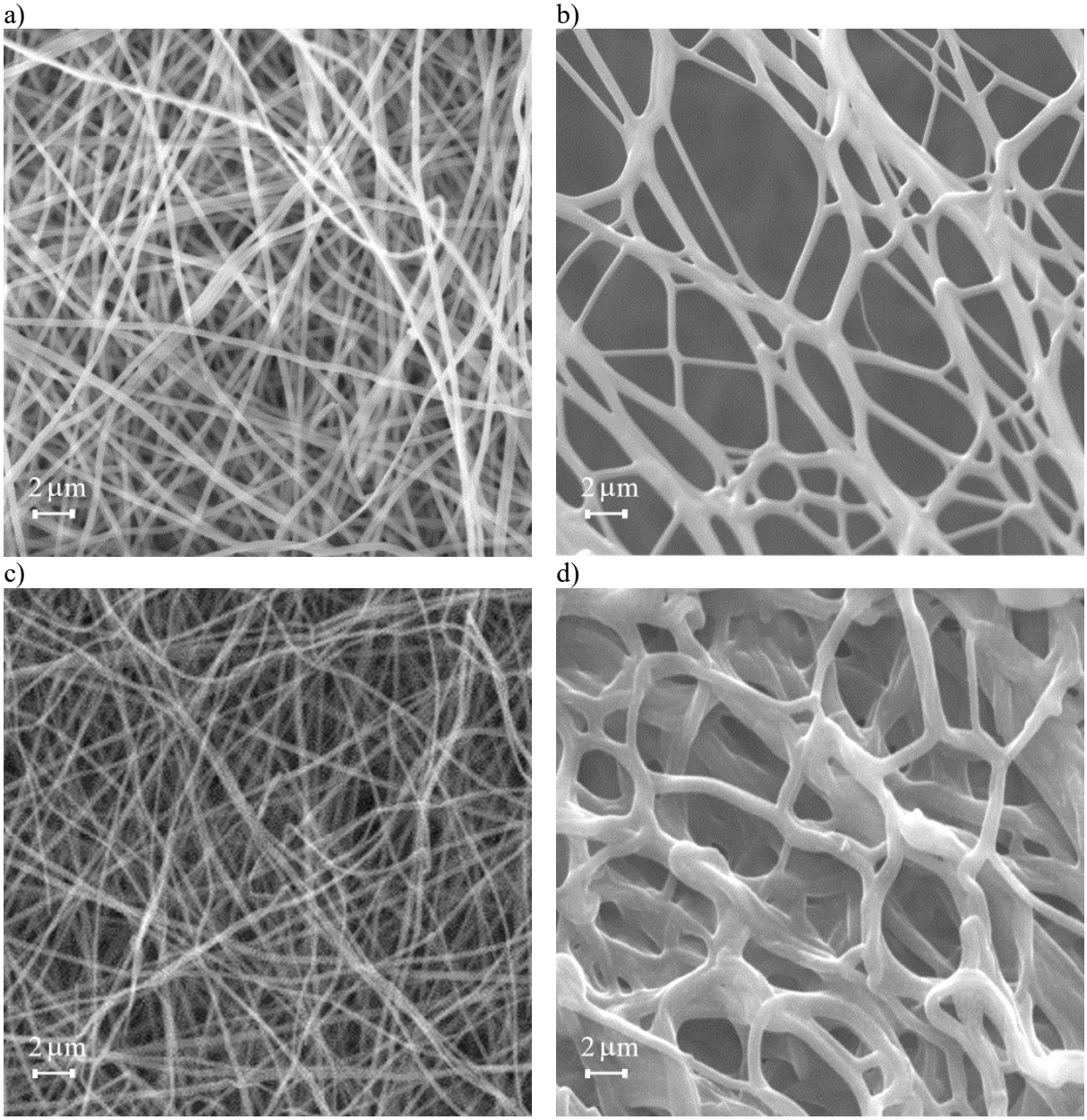

Fig. S6. SEM micrographs of PVP (a,b) and silver (c, d), copper (e, f) and zinc (g, h) loaded mats (M) after crosslinking (left column, a, c, e, and g) and after water immersion (right column, b, d, f, and h).

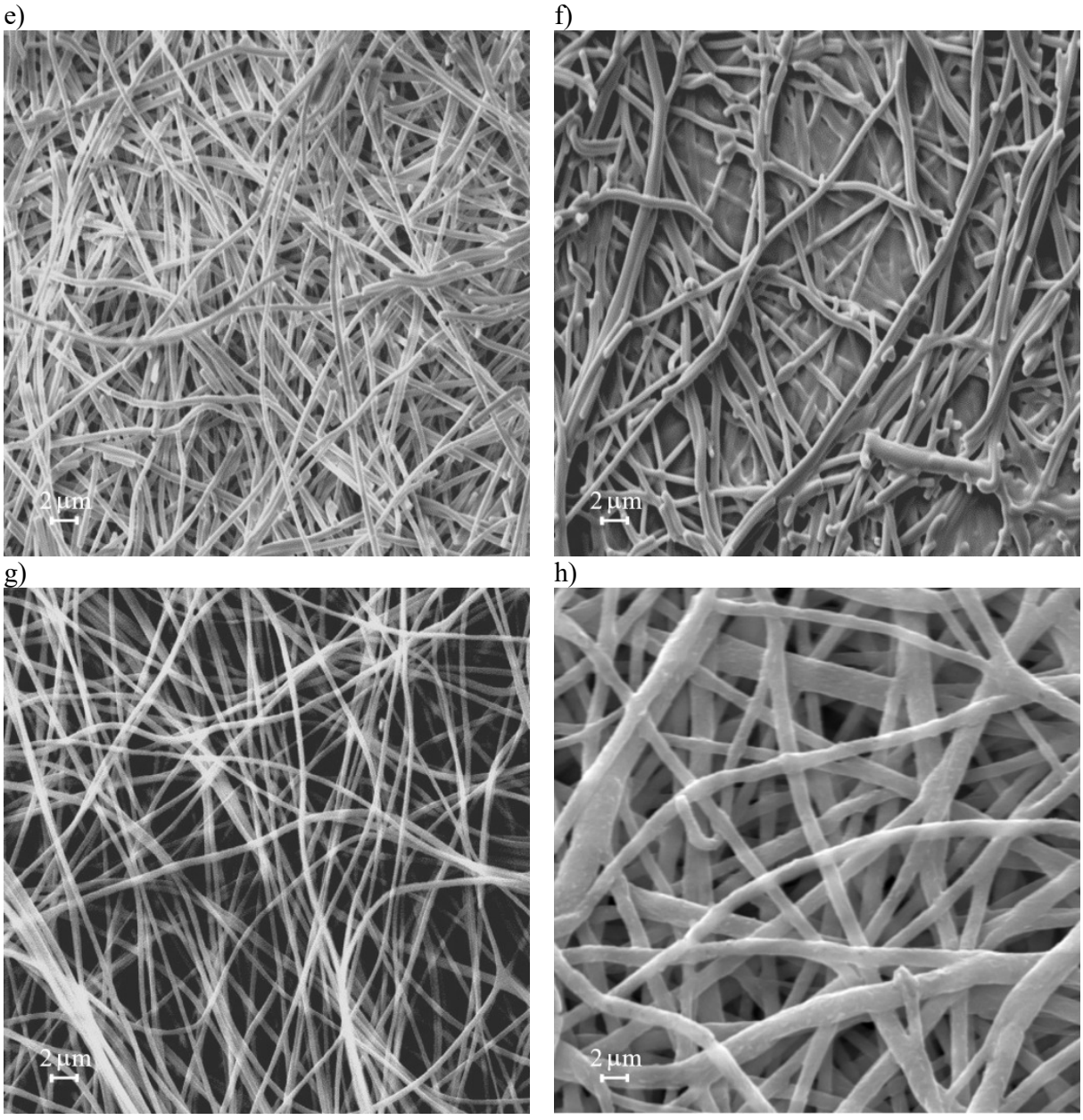

Fig. S6 (cont.). SEM micrographs of PVP (a,b) and silver (c, d), copper (e, f) and zinc (g, h) loaded mats (M) after crosslinking (left column, a, c, e, and g) and after water immersion (right column, b, d, f, and h).

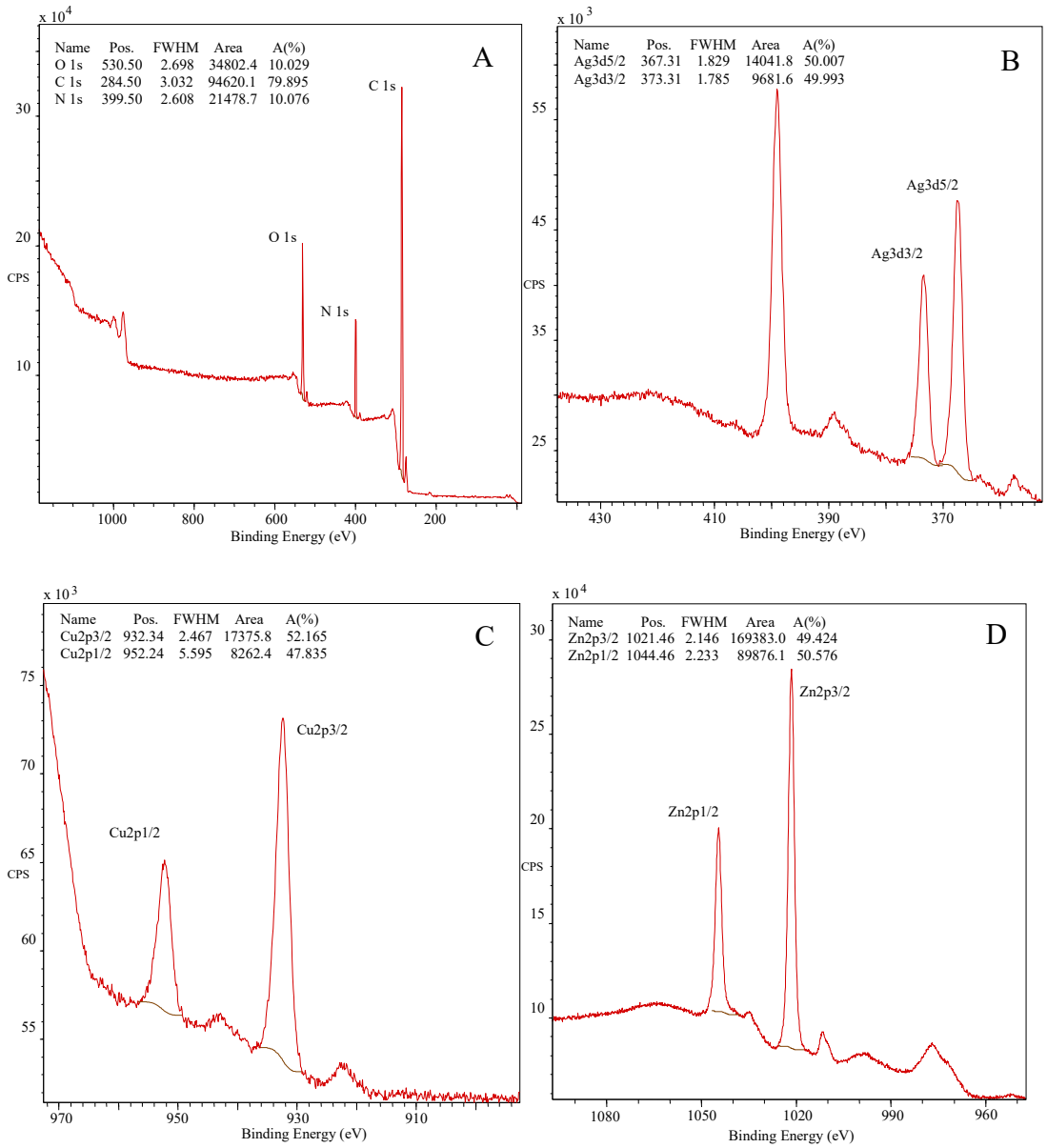

Fig. S7. XPS spectra of PVP (A) and metal loaded mats: Ag (B), Cu (C) and Zn (D).